

A Multimode Antenna Design with Polarization Diversity

Kai Zhang¹, Ping Jack Soh², Mingjun Wang¹, and Sen Yan³

¹ School of Automation and Information Engineering, Xi'an University of Technology, Xi'an 710048, China, kai.zhang@xaut.edu.cn

² Centre for Wireless Communications (CWC), University of Oulu, 90570 Oulu, Finland, Pingjack.Soh@oulu.fi

³ School of Information and Communications Engineering, Xi'an Jiaotong University, Xi'an 710049, China, sen.yan@xjtu.edu.cn

Abstract—In this article, a multimode antenna with polarization diversity is designed for smartwatch applications. The antenna structure consists of a circular watch frame and a circuit mainboard. Two ports are used to excite the antenna in odd and even modes, and polarization-diversity resonances are achieved. Additionally, a circular current is excited on one port to realize low-frequency multimode operation. Furthermore, high-order modes are excited by introducing slots in the circuit board, enabling multiband and multimode operation. The port 1 is working at 2.45 GHz, 4.1 GHz, and 5.8 GHz. And Port 2 works at 0.82 GHz, 2.45 GHz, 4.1 GHz, and 5.8 GHz for ISM band. The proposed antenna exhibits stable radiation patterns and high port isolation across multiple frequency bands, making it a promising candidate for next-generation smartwatch devices.

Index Terms—multimode antenna, polarization diversity, smartwatch, wearable antenna.

I. INTRODUCTION

With the progress in Internet of Things (IoT) technologies, Wireless Body Area Networks (WBANs) have become essential local area networks for communication on and around the human body [1-3]. In healthcare monitoring and communication, WBANs are increasingly important. Smartwatches, designed as wearable devices for wrist-based communication and monitoring, have gained significant popularity due to their intelligence, convenience, and ability to connect personal endpoints with remote networks effortlessly. Common functionalities of a smartwatch include blood oxygen level tracking, activity monitoring, emergency communications, internet access, body temperature measurement, heartbeat tracking, location services, and electrocardiogram (ECG) readings [4, 5].

The design of watch antennas can be categorized into four types based on their placement: frame antenna design [1, 6-11], mainboard antenna design [12-17], strap antenna design [18-20], and screen antenna design [21-23]. Each type is specifically tailored to meet distinct functionalities and requirements. Additionally, innovative methods and technologies are being applied in smartwatch antenna designs. Characteristic mode analysis serves as an effective technique for examining orthogonal modes and multi-mode distributions [1, 9, 12]. This method's strength lies in its capacity to analyze the overall structure of the antenna without compromising performance when additional components are integrated into the watch. All analyzed modes remain orthogonal which aids in designing extra features like circular polarization or

polarization diversity. However, it has limitations since it only evaluates existing structures requiring trials with structural modifications for specific patterns. Electromagnetic metamaterials represent another advanced approach for designing wearable antennas [6, 16, 17, 24-26]. Previous studies have leveraged unique electromagnetic properties of these materials to create Electromagnetic Band Gap (EBG) reflectors that minimize size while lowering resonance frequencies, thus enhancing performance. However, when such antennas are fully integrated within the watch case, their radiation efficiency may be impacted once assembled.

To improve functionality while addressing multi-band communication needs within wearable technology designs incorporate techniques such as parasitic elements [1], electromagnetic metamaterials [6], stacking antennas [8], and differential feeding [26]. These strategies allow wearable antennas to efficiently operate across various frequency bands catering effectively to modern smartwatch application demands.

This paper proposes a multimode watch antenna utilizing electric field coupling alongside magnetic field coupling feeding methods. To achieve this polarization diversity dual-port feeding structure generate current directions that are orthogonal along the watch frame operating at 2.5 GHz, and 5.8 GHz respectively. Then, integrating motherboard along with frame results in even full-wave mode configuration working at 4.1 GHz creating dual-port quadruple-band co-polarization diversity watch antenna. In addition, feeding structure of port 2 generates a circuit tuning, and its resonance frequency is 0.82 GHz. Ultimately, the proposed antenna can generate tri-band polarization diversity radiation and work at four frequencies, greatly reducing polarization attenuation caused by human movement and multipath effects caused by the environment. This antenna will be a good choice for multi-functional smartwatch antennas.

II. ANTENNA DESIGN

A. Antenna Configuration

The proposed smartwatch antenna consists of two primary components: the watch frame and the mainboard. The layered structure of these components is depicted in Fig. 1(a). The watch frame is constructed from a metal plating applied to the exterior side of a circular substrate with a thickness of 1 mm. This substrate has a permittivity of 4.3 and a loss tangent of

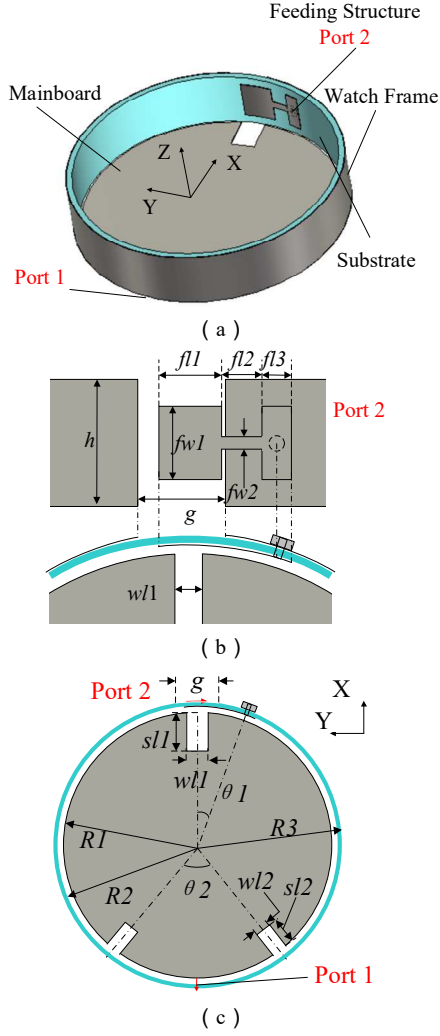


Fig. 1. The model of the proposed antenna. (a) three-dimensional view, (b) feeding structure, (c) top view.

TABLE I DIMENSIONS OF THE ANTENNA

$fl1$	$fl2$	$fl3$	$fw1$	$fw2$	h
5.6 mm	3.0 mm	2.4 mm	6.9 mm	1.2 mm	10.0 mm
g	$wl1$	$wl2$	$sl1$	$sl2$	$R1$
6.8 mm	4.3 mm	2.4 mm	5.9 mm	4.0 mm	22.7 mm
$R2$	$R3$	$\theta1$	$\theta2$		
23.0 mm	24.0 mm	20.7°	40.0°		

0.025. A patch structure (designated as port 2) is affixed to the inner surface of the circular support to excite the slot in the watch frame. On the opposite side of the symmetry axis, a connector (port 1) links the metallic portion of the mainboard to the exterior of the frame, facilitating the feeding of the watch antenna. The dimensions of the ring structure measure $\pi \times 24.0 \times 24.0 \times 10$ mm³. The specific dimensions of the proposed antenna, as shown in Fig. 1(b) and (c), are detailed in Table I. The design was stacked and optimized using CST Microwave Studio.

B. Working Principles

The current distribution of the antenna modes is shown in Fig. 2 and 3, which indicates the working principle. From the current distribution in Fig. 2, it can be seen that when the port

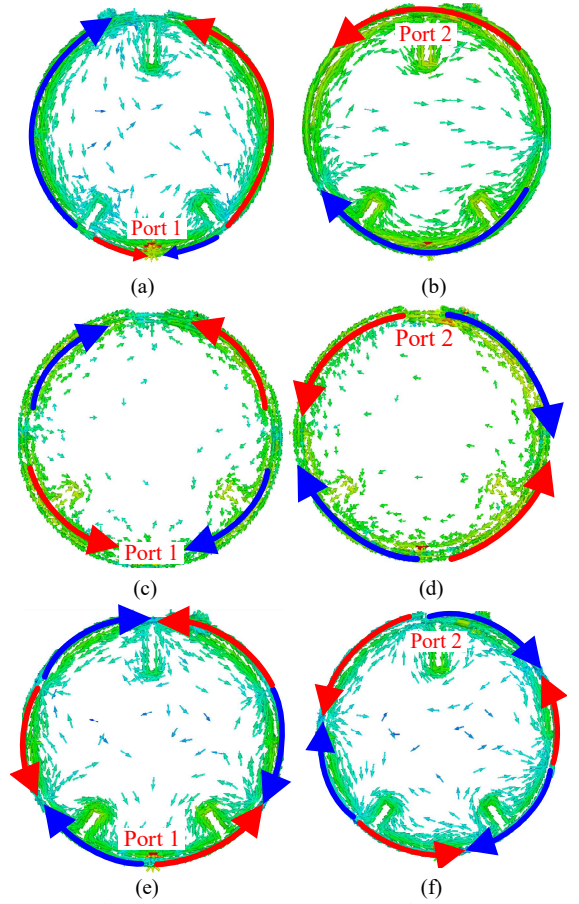


Fig. 2. Current distributions. (a) Port 1, 2.45 GHz, (b) Port 2, 2.45 GHz, (c) Port 1, 4.1 GHz, (d) Port 2, 4.1 GHz, (e) Port 1, 5.8 GHz, and (f) Port 2, 5.8 GHz.

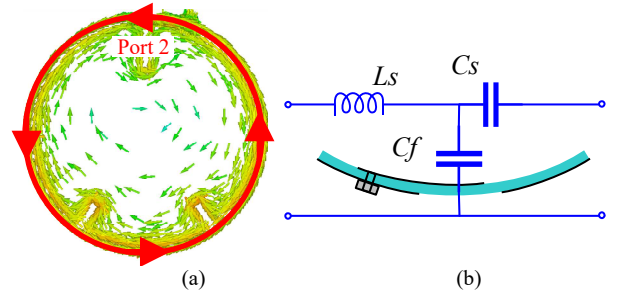


Fig. 3. (a) Current distribution at 0.82 GHz, and (b) its equivalent circuit.

1 is excited, the circuit shows vertical symmetry. Therefore, the watch frame can be analyzed symmetrically with the middle being the magnetic wall. The watch frame can be regarded as an equivalent transmission line in the equivalent circuit. Similarly, when the port 2 is excited, the circuit shows horizontal symmetry at 2.45 GHz. Thus three resonant modes are generated from the harmonic of the equivalent transmission line. Meanwhile, coupling feeding is performed at port 2 to generate a current distribution orthogonal to that of port 1. The 4.1 GHz of port 1 and port 2 forms four out-of-phase half-wave periodic currents flowing along the circumference on the watch frame, and the current distribution at zero phase is shown in Fig. 2. Ports 1 and 2 at 5.8 GHz are

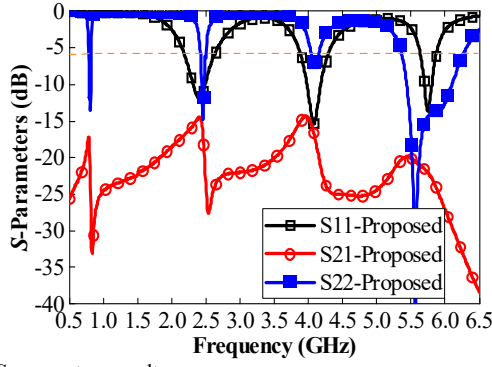


Fig. 4. S-parameters results.

symmetrical fourth-order modes, and their current distributions at zero phase are shown in Table II. The matching at high frequencies can be adjusted through the slots on the main board.

For 0.82 GHz at port 2, a tuning circuit is generated at the slot feeding point as shown in Fig. 3(b), and the resonant impedance is

$$Z_{\text{feed}} = \frac{1 - \omega^2 L_s C_s}{j\omega C_s + j\omega C_f (1 - \omega^2 L_s C_s)}. \quad (1)$$

Therefore, the lowest resonant frequency can be obtained by

$$f_{p2} = \frac{1}{2\pi\sqrt{L_s C_s}}, \quad (2)$$

where L_s is the equivalent inductance of the watch frame, C_s is the equivalent capacitance of the slot on the watch frame, and C_f is the equivalent capacitance between the feeding patch and watch frame. The resonant mode will change with the parameters of this circuit. Due to the generation of circuit tuning on the watch frame, the current distribution is a clockwise circular flow as shown in Fig. 3(a). But the disadvantage is that the resonant point bandwidth of the tuning circuit is relatively narrow.

III. RESULTS AND DISCUSSION

As shown in Fig. 4, the simulation results of the S parameters of the antenna designed in this paper are presented. Due to the narrow low-frequency bandwidth, a reflection coefficient less than -6 dB (VSWR < 3) is adopted as the performance evaluation criterion. The three frequency bands 2.45 GHz, 4.1 GHz, and 5.8 GHz of port 1 S_{11} are 2.19~2.62 GHz with 434 MHz bandwidth, 3.89~4.29 GHz with 400 MHz, and 5.64~5.87 GHz with 230 MHz bandwidth. For S_{22} of port 2, the four frequency bands are 0.788~0.825 GHz with 37 MHz, 2.42~2.5 GHz with 80 MHz, 4.04~4.15 GHz with 110 MHz, and 5.36~6.26 GHz with 900 MHz, respectively. The isolation between two ports are under -15 dB over the working frequency band.

In Fig. 5, the simulated far-field patterns of the antenna in the four frequency bands are presented. The radiation patterns of 0.82 GHz, 4.4 GHz, and 5.8 GHz present a petal-shaped configuration, mainly due to the reverse current on the watch frame, and the specific analysis has been described in the

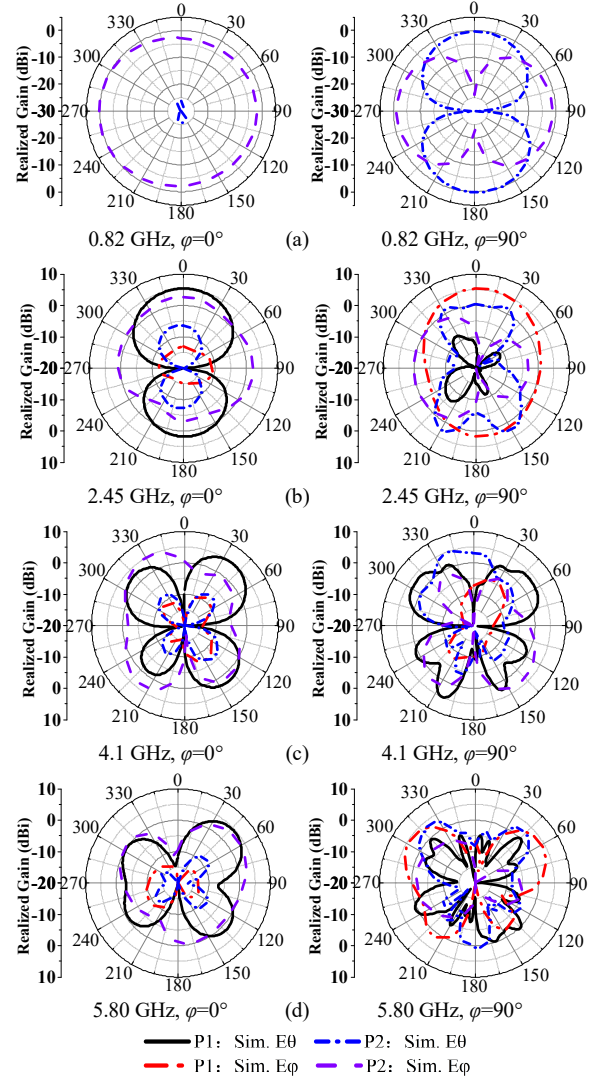


Fig. 5. The pattern of the port 1 and port 2. (a) 0.82 GHz, (b) 2.45 GHz, (c) 4.1 GHz, and (d) 5.8 GHz.

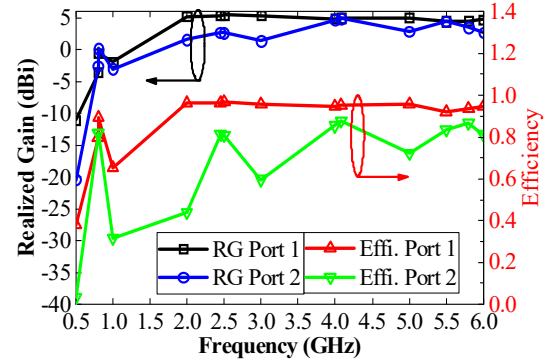


Fig. 6. Realized gain and efficiency of the antenna.

working principle section. In Fig. 5 (a), the resonance at 0.82 GHz is circuit tuned, thus presenting an electrically small loop radiation mode.

Furthermore, the simulation of the far-field gain and efficiency of the antenna were conducted, and the results are shown in Fig. 6. The simulation results of port 1/port 2 in the three frequency bands (i.e., 2.45 GHz, 4.1 GHz, and 5.8 GHz)

are 5.40 dBi/2.71 dBi, 5.01 dBi/4.91 dBi, and 4.50 dBi/3.50 dBi, respectively. The efficiency is 96%/81%, 95%/88%, and 94%/87%, respectively. At 0.82 GHz in port 2, the realized gain is 0.2 dBi and the efficiency is 82%. The efficiency difference between port 1 and port 2 is mainly due to the difference in feeding mode, port 1 is fed directly, while port 2 is fed through coupling. Coupled feeding structure need to consider the loss of the substrate of the watch frame.

IV. CONCLUSION

This paper presents a multimode antenna for smartwatches that employs both electric and magnetic field coupling feeding techniques. To achieve polarization diversity, the dual-port feeding design creates orthogonal current directions along the watch frame, operating at frequencies of 2.5 GHz, 4.1 GHz, and 5.8 GHz. Additionally, the feeding structure of port 2 facilitates circuit tuning with a resonance frequency of 0.82 GHz. The proposed antenna demonstrates consistent radiation patterns and excellent port isolation across various frequency bands, positioning it as a strong candidate for future smartwatch technologies.

ACKNOWLEDGMENT

This work was supported in part by the National Key Research and Development Program of China under Grant 2020YFA0709800; in part by the Academy Research Fellowship ULTRAGRAM under Grant 355643 by the Research Council of Finland; in part by National Natural Science Foundation of China under Grant 92052106; and in part by Shaanxi Provincial University Innovation Team and Xi'an Key Industrial Chain Critical Core Technology Research Project under Grant 103-433023062.

REFERENCES

- [1] B. Xiao, H. Wong, D. Wu, and K. L. Yeung, "Design of Small Multiband Full-Screen Smartwatch Antenna for IoT Applications," *IEEE Internet Things J.*, vol. 8, no. 24, pp. 17724-17733, 2021.
- [2] K. Zhang, P. J. Soh, J. Chen, and S. Yan, "CRLH TL-Based Compact Wideband Button Antenna for Biomedical Applications," *IEEE Journal of Electromagnetics, RF and Microwaves in Medicine and Biology*, vol. 8, no. 1, pp. 68-77, 2024.
- [3] Z. Luo, Q. Zhang, W. Wang, and T. Jiang, "Single-Antenna Device-to-Device Localization in Smart Environments With Backscatter," *IEEE Internet Things J.*, vol. 9, no. 12, pp. 10121-10129, 2022.
- [4] K. Zhang, P. J. Soh, and S. Yan, "Meta-Wearable Antennas-A Review of Metamaterial Based Antennas in Wireless Body Area Networks," *Materials*, vol. 14, no. 1, pp. 1-20, Jan 2021.
- [5] K. Zhang, P. J. Soh, and S. Yan, "Design of a Compact Dual-Band Textile Antenna Based on Metasurface," *IEEE Trans. Biomed. Circuits Syst.*, vol. 16, no. 2, pp. 211-221, Apr 2022.
- [6] B. Wang, S. Yan, and Y. He, "A CRLH-TL Inspired Dual-Band Antenna With Polarization Diversity for Wrist-Worn Wireless Body Area Network Devices," *IEEE Trans. Antennas Propag.*, vol. 71, no. 6, pp. 4812-4822, 2023.
- [7] B. Wang and S. Yan, "Design of Smartwatch Integrated Antenna With Polarization Diversity," *IEEE Access*, vol. 8, pp. 123440-123448, 2020.
- [8] C. T. Liao, Z. K. Yang, and H. M. Chen, "Multiple Integrated Antennas for Wearable Fifth-Generation Communication and Internet of Things Applications," *IEEE Access*, vol. 9, pp. 120328-120346, 2021.
- [9] D. Wen, Y. Hao, H. Wang, and H. Zhou, "Design of a MIMO Antenna With High Isolation for Smartwatch Applications Using the Theory of Characteristic Modes," *IEEE Trans. Antennas Propag.*, vol. 67, no. 3, pp. 1437-1447, 2019.
- [10] D. Wu and S. W. Cheung, "A Cavity-Backed Annular Slot Antenna With High Efficiency for Smartwatches With Metallic Housing," *IEEE Trans. Antennas Propag.*, vol. 65, no. 7, pp. 3756-3761, 2017.
- [11] S. W. Su and Y. T. Hsieh, "Integrated Metal-Frame Antenna for Smartwatch Wearable Device," *IEEE Trans. Antennas Propag.*, vol. 63, no. 7, pp. 3301-3305, 2015.
- [12] X. Zhang *et al.*, "Analysis and Design of Stable-Performance Circularly-Polarized Antennas Based on Coupled Radiators for Smart Watches," *IEEE Trans. Antennas Propag.*, vol. 70, no. 7, pp. 5312-5323, 2022.
- [13] R. Rabhi, S. Gahgouh, and A. Gharsallah, "Watchstrap integrated wideband circularly polarized antenna design for smartwatch applications," (in English), *IET Microw. Antennas Propag.*, vol. 16, no. 9, pp. 587-601, Jul 2022.
- [14] S. Kumar *et al.*, "A Bandwidth-Enhanced Sub-GHz Wristwatch Antenna Using an Optimized Feed Structure," *IEEE Antennas Wirel. Propag. Lett.*, vol. 20, no. 8, pp. 1389-1393, 2021.
- [15] Y. S. Chen and T. Y. Ku, "A Low-Profile Wearable Antenna Using a Miniature High Impedance Surface for Smartwatch Applications," *IEEE Antennas Wirel. Propag. Lett.*, vol. 15, pp. 1144-1147, 2016.
- [16] D. Rano and M. Hashmi, "Extremely compact EBG-backed antenna for smartwatch applications in medical body area network," *IET Microw. Antennas Propag.*, vol. 13, no. 7, pp. 1031-1040, Jun 12 2019.
- [17] G. Li, G. Gao, J. Bao, B. Yi, C. Song, and L. a. Bian, "A Watch Strap Antenna for the Applications of Wearable Systems," *IEEE Access*, vol. 5, pp. 10332-10338, 2017.
- [18] A. Abdelhakim, M. Cabedo-Fabrés, and M. F. Bataller, "PIFA antenna for smart watch application in the 2.4 GHz band," in *2021 IEEE International Symposium on Antennas and Propagation and USNC-URSI Radio Science Meeting (APS/URSI)*, 2021, pp. 703-704.
- [19] Y. Jia, L. Liu, J. Hu, and L. J. Xu, "Miniaturized wearable watch antenna for wristband applications," in *2019 IEEE MTT-S International Microwave Biomedical Conference (IMBioC)*, 2019, vol. 1, pp. 1-3.
- [20] W. Hong, S. Ko, Y. G. Kim, and S. Lim, "Invisible antennas using mesoscale conductive polymer wires embedded within OLED displays," in *2017 11th European Conference on Antennas and Propagation (EUCAP)*, 2017, pp. 2809-2811.
- [21] W. Hong, S. Lim, S. Ko, and Y. G. Kim, "OLED-embedded antennas for 2.4 GHz Wi-Fi and bluetooth applications," in *2017 IEEE International Symposium on Antennas and Propagation & USNC/URSI National Radio Science Meeting*, 2017, pp. 2551-2552.
- [22] W. Hong, S. Lim, S. Ko, and Y. G. Kim, "Optically Invisible Antenna Integrated Within an OLED Touch Display Panel for IoT Applications," *IEEE Trans. Antennas Propag.*, vol. 65, no. 7, pp. 3750-3755, 2017.
- [23] K. Zhang, M. Särestöniemi, S. Myllymäki, P. J. Soh, J. Chen, and S. Yan, "A Wideband Circularly Polarized Antenna With Metasurface Plane for Biomedical Telemetry," *IEEE Antennas Wirel. Propag. Lett.*, vol. 23, no. 6, pp. 1879-1883, 2024.
- [24] K. Zhang, P. J. Soh, T. Wu, M. Wang, and S. Yan, "A Compact Multi-Mode Antenna Design Based on Metasurface for Wideband Applications," *IEEE Trans. Antennas Propag.*, vol. 72, no. 8, pp. 6747-6752, 2024.
- [25] K. Zhang, G. A. E. Vandenbosch, and S. Yan, "A Novel Design Approach for Compact Wearable Antennas Based on Metasurfaces," *IEEE Trans. Biomed. Circuits Syst.*, vol. 14, no. 4, pp. 918-927, 2020.
- [26] B. Cheng, Z. Du, and D. Huang, "A Differentially Fed Broadband Multimode Microstrip Antenna," *IEEE Antennas Wirel. Propag. Lett.*, vol. 19, no. 5, pp. 771-775, 2020.